Supporting Information

Phosphorescent Acyclic Cucurbituril Solid Supramolecular Multicolour Delayed Fluorescence Behaviour

Man Huo, Shuang-Qi Song, Xian-Yin Dai, Fan-Fan Li, Yu-Yang Hu and Yu Liu*

[*] Dr. M. Huo, S.-Q Song, X. -Y Dai, F.-F Li, Y.-Y. Hu Prof. Dr. Yu Liu

College of Chemistry, State Key Laboratory of Elemento-Organic Chemistry Nankai University,

Tianjin 300071, P. R. China

E-mail: yuliu@nankai.edu.cn

Table of Content

Section A. Instrumentation and Methods…..S3

Section B. Synthetic Protocols…..S4

Section C. Photophysical Properties of ACB-COOH.…..S8

Section D. Host-Guest Properties of ACB-COOH and RhB, PyY or Mor.…..S22

Section E. Characterizations of Photoinduced Electron Transfer (PET) Process of Mor⊂ACB-COOH film.…..S27

Section F. Characterizations of Phosphorescence Energy Transfer Behaviors of RhB⊂ACB-COOH or PyY⊂ACB-COOH film.…..S28

Section G. References…..S31

Section A. Instrumentation and Methods

All reagents and solvents were obtained from commercial suppliers and were used as supplied, unless otherwise noted. Column chromatography was performed on 200-300 mesh silica gel. NMR spectra were recorded on a Bruker AV400 spectrometer or AV600 spectrometer. High-resolution MS was performed on a QFT-ESI. UV-vis absorption spectra were recorded on a Shimadzu UV-3600 spectrophotometer with a PTC-348WI temperature controller in a quartz cell (light path 10 mm) at 298 K. Photoluminescence spectra, lifetime and quantum efficiency were obtained on FLS5 instrument (Edinburg Instruments, Livingstone, UK). Temperature-dependent spectra were obtained on FLS1000 instrument (Edinburg Instruments, Livingstone, UK). The Fourier transform infrared spectra were processed on Tensor II (Bruker). All measurements were carried out at room temperature (RT) except for specifying otherwise.

General preparation for the ACB-COOH@PVA film: ACB-COOH (10 mg) was added to 1 mL water and added moderate $NH_3 \cdot H_2O$ to ensure complete dissolution of ACB-COO^-. The mixture was stirred until completely dissolved and then added with a quantitative amount of PVA solution (60 mg/mL). After removing the air bubbles by ultrasound, the mixture was dropped onto the quartz sheet. Films were obtained after thorough drying.

General preparation for the Guest⊂ACB-COOH@PVA film: ACB-COOH (10 mg) was added to 1 mL water and added moderate $NH_3 \cdot H_2O$ to ensure complete dissolution of ACB-COO^-, and then added a quantitative amount of guest aqueous solution. The mixture was stirred until completely dissolved and then added with a quantitative amount of PVA solution (60 mg/mL). After removing the air bubbles by ultrasound, the mixture was dropped onto the quartz sheet. Films were obtained after thorough drying.

Section B. Synthetic Protocols

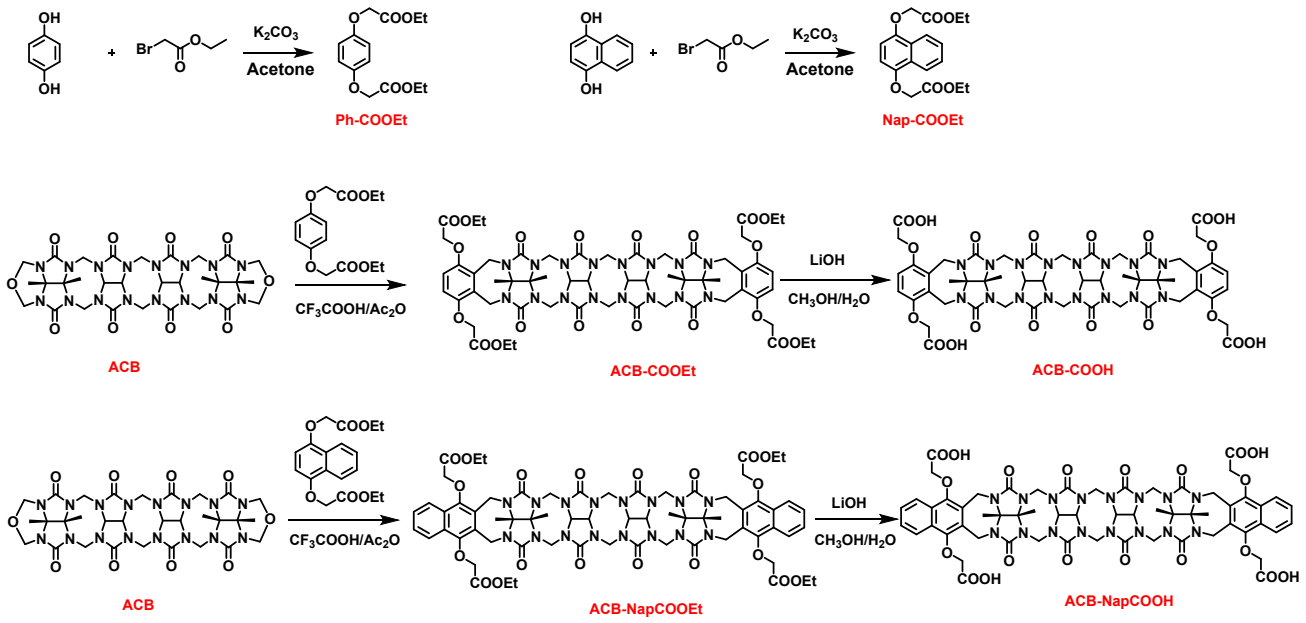

Scheme S1. Synthetic routes of ACB-COOH, ACB-NapCOOH.

Compound ACB, Ph-COOEt, Nap-COOEt, ACB-COOH, ACB-NapCOOH were prepared according to the literature[1-4].

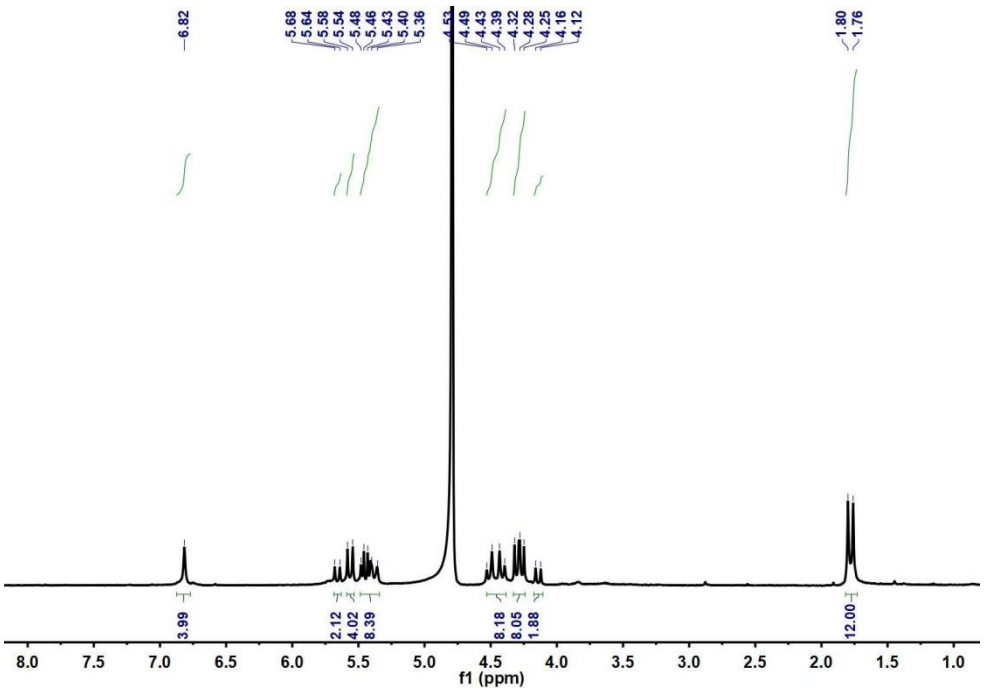

Fig. S1 ^{1}H NMR spectrum (600 MHz, D_2O, 298 K) of ACB-COOH.

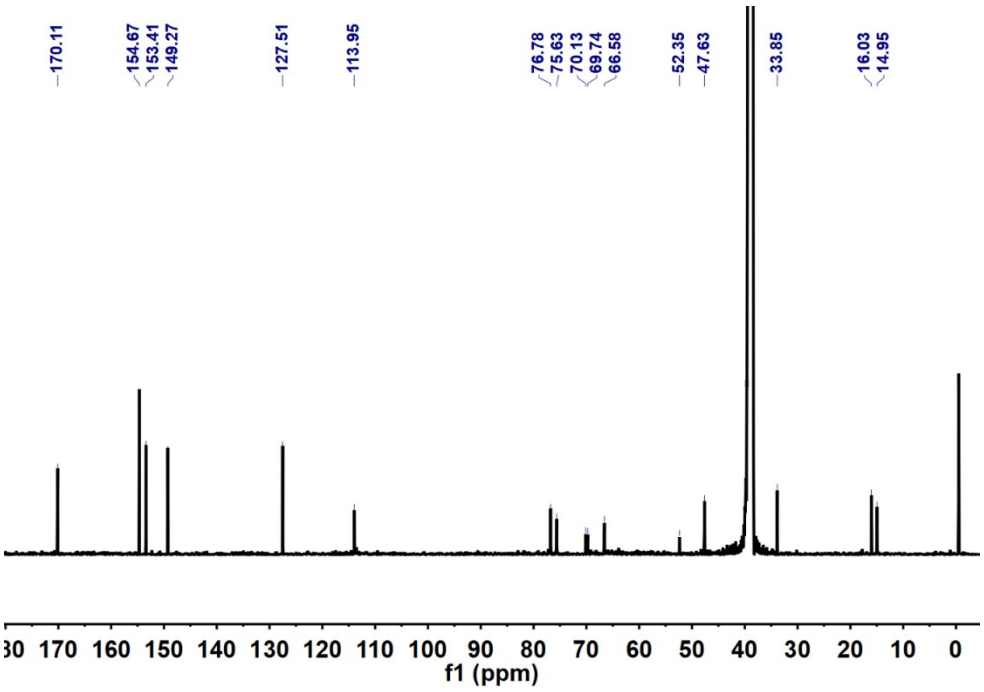

Fig. S2 ^{13}C NMR spectrum (100 MHz, DMSO-d_6, 298 K) of ACB-COOH.

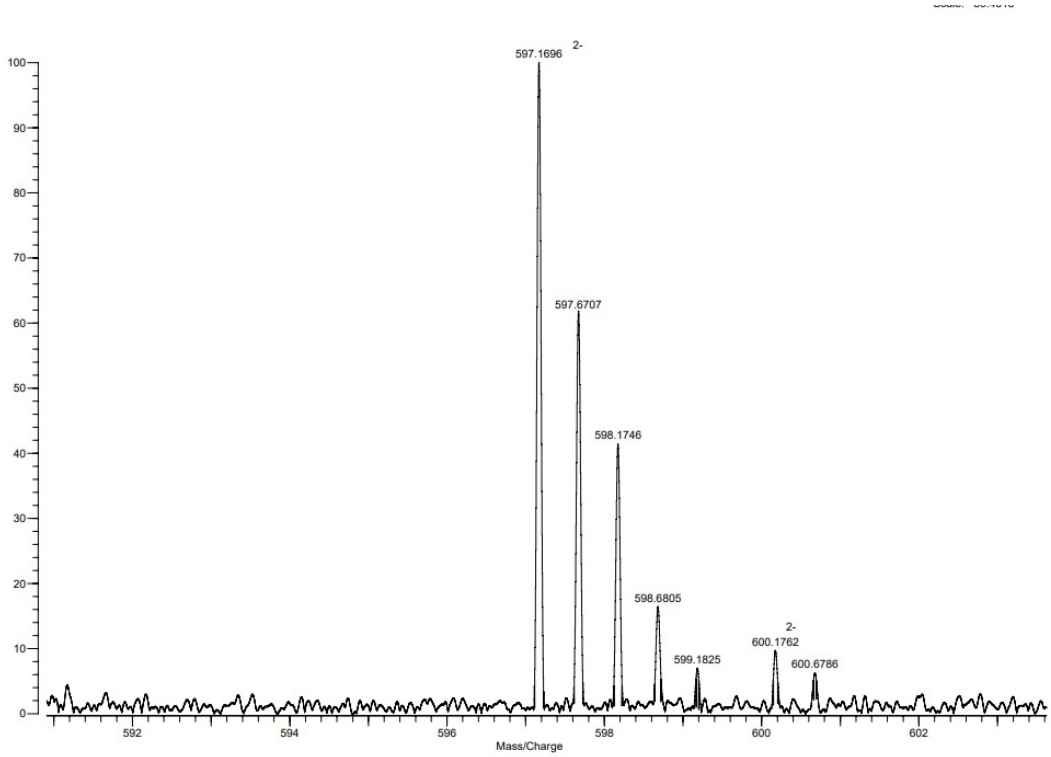

Fig. S3 HR-MS spectrum of ACB-COOH.

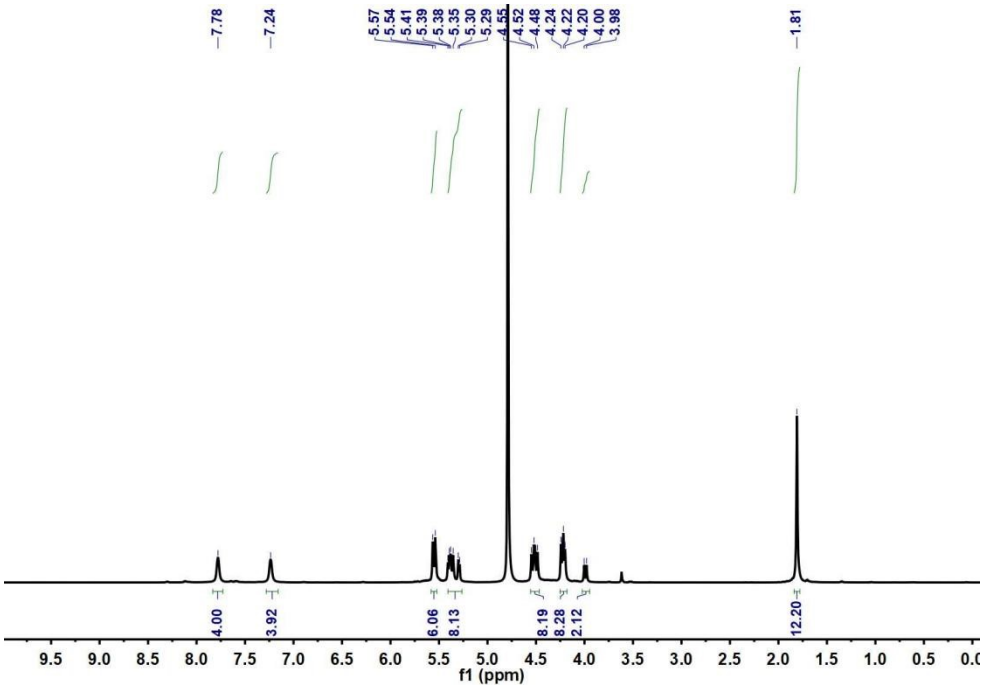

Fig. S4 ^{1}H NMR spectrum (600 MHz, D_2O, 298 K) of ACB-NapCOOH.

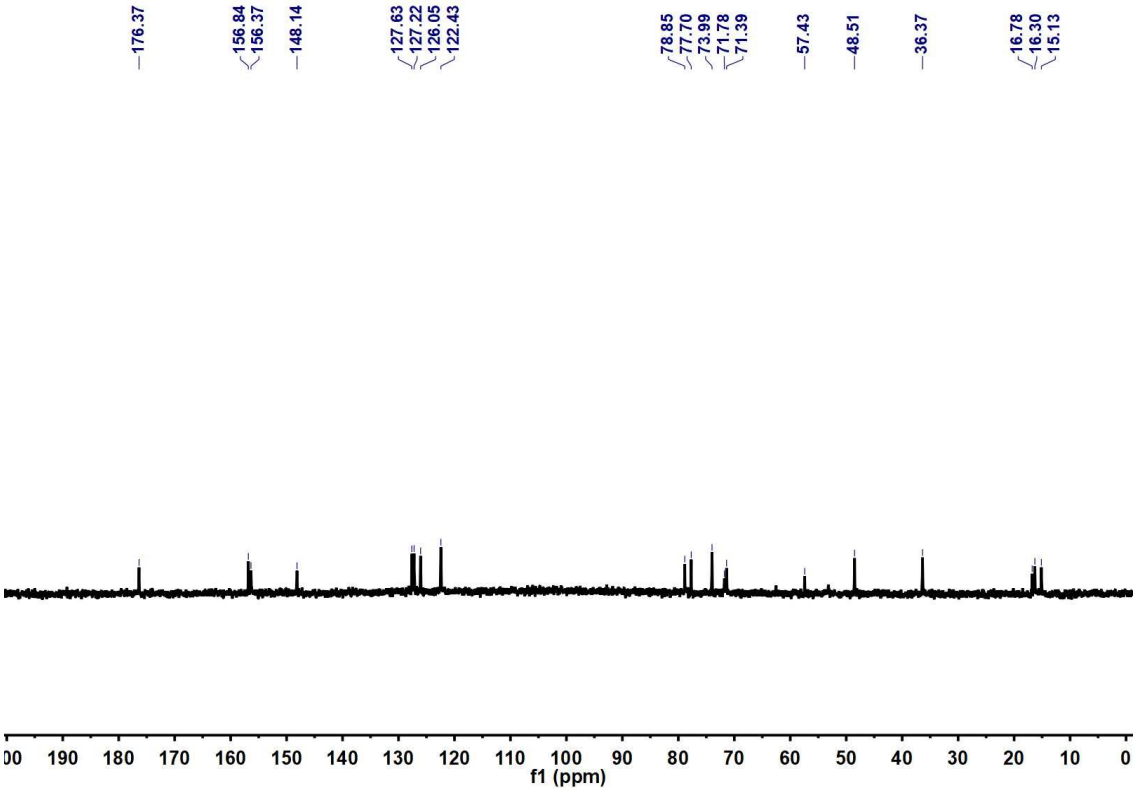

Fig. S5 ^{13}C NMR spectrum (100 MHz, DMSO-d_6, 298 K) of ACB-NapCOOH.

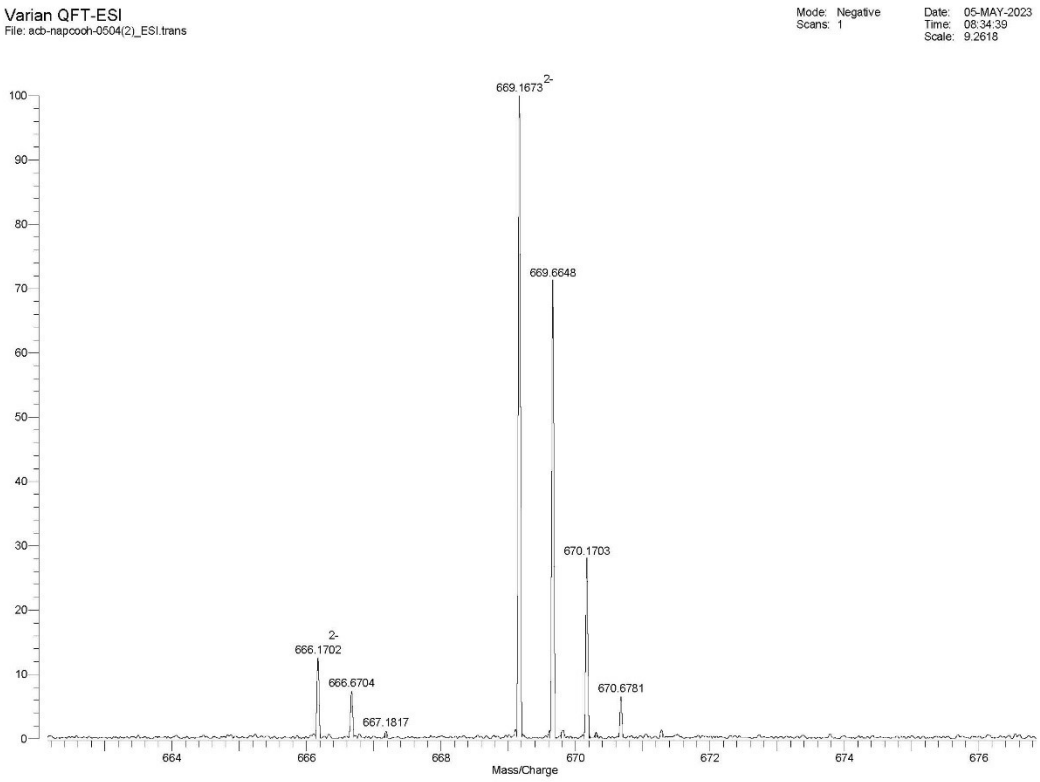

Fig. S6 HR-MS spectrum of ACB-NapCOOH.

Section C. Photophysical Properties of ACB-COOH.

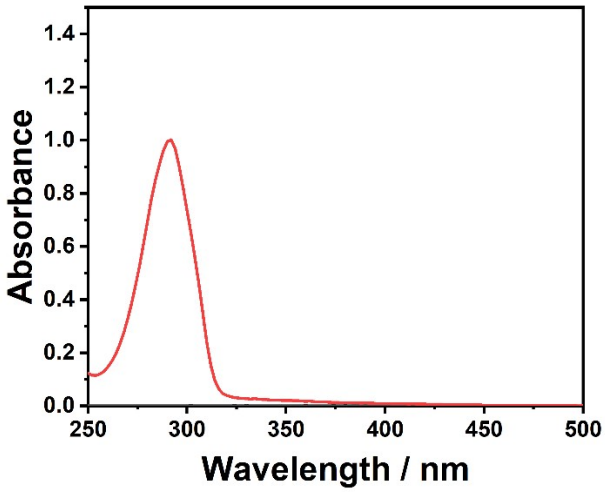

Fig. S7 The UV–vis absorption spectrum of ACB-COOH in aqueous solution.

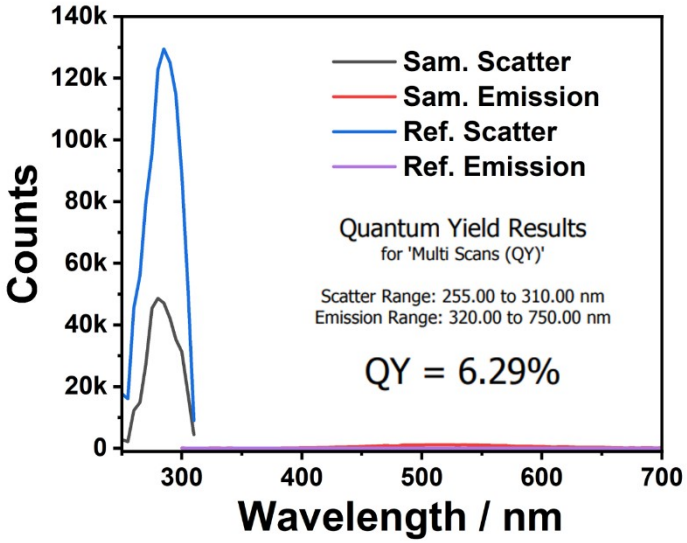

Fig. S8 The quantum yield of ACB-COOH.

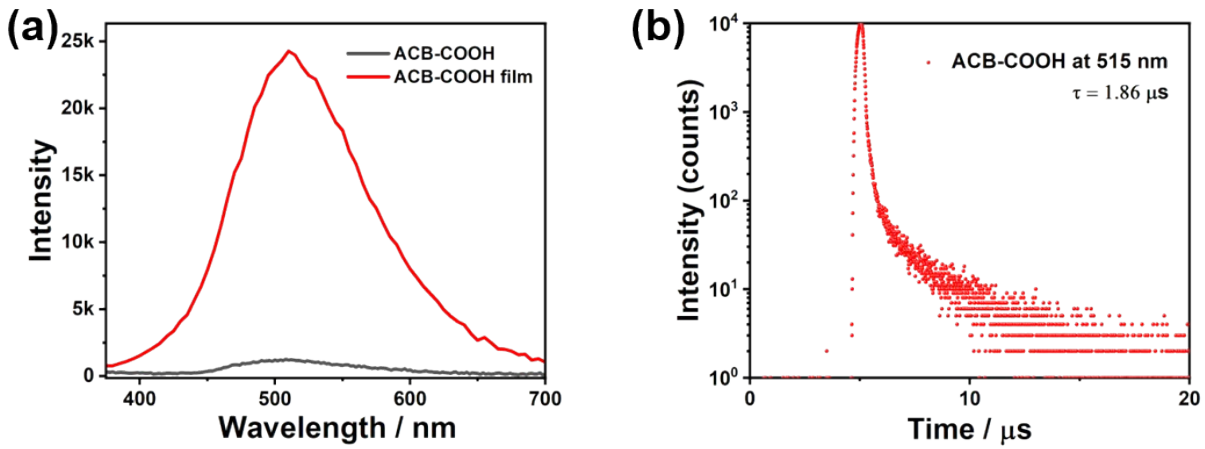

Fig. S9 a) Phosphorescence emission spectra of ACB-COOH powder and ACB-COOH film. b) The time-resolved PL decay spectrum of ACB-COOH powder at 515 nm.

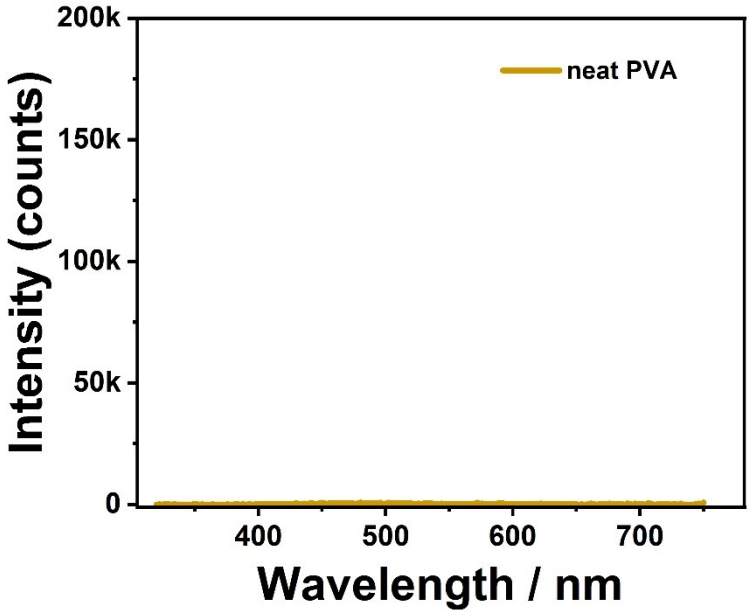

Fig. S10 Phosphorescence emission spectrum of neat PVA film.

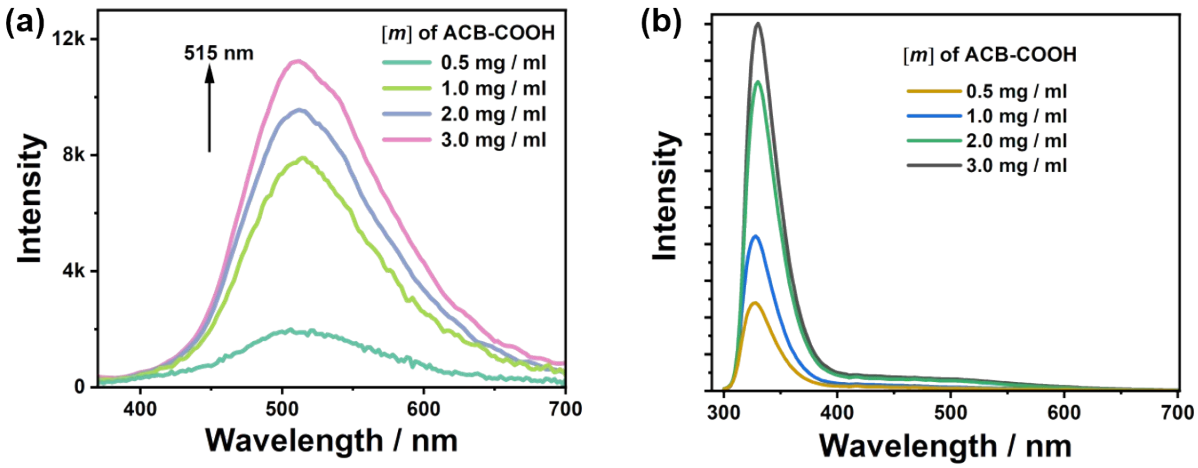

Fig. S11 (a) Phosphorescence intensity, (b) photoluminescence intensity excited at 280 nm for ACB-COOH-doped PVA with different doping concentration [*m*].

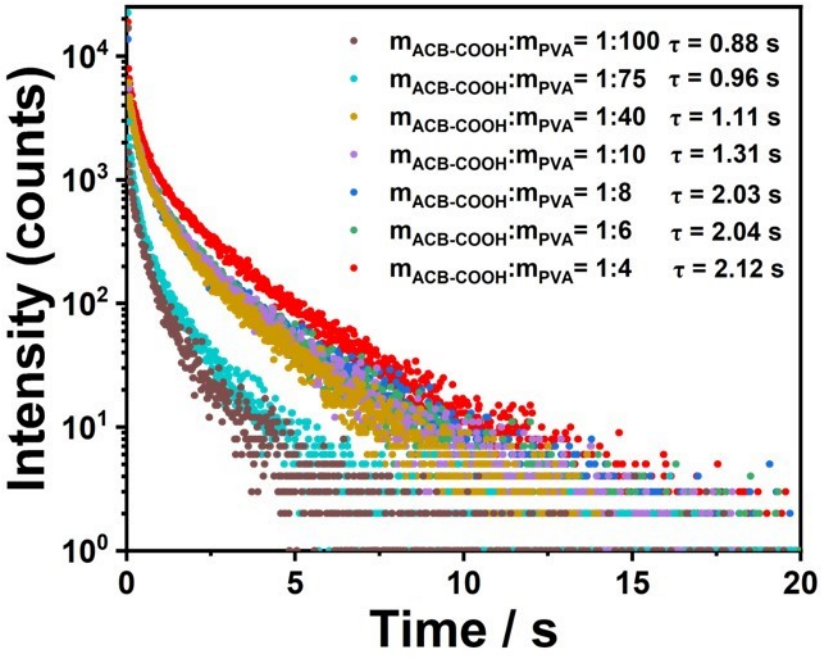

Fig. S12 Lifetime decay curves of phosphorescence emission band at 510 nm for ACB-COOH-doped PVA with different ACB-COOH/PVA mass ratio.

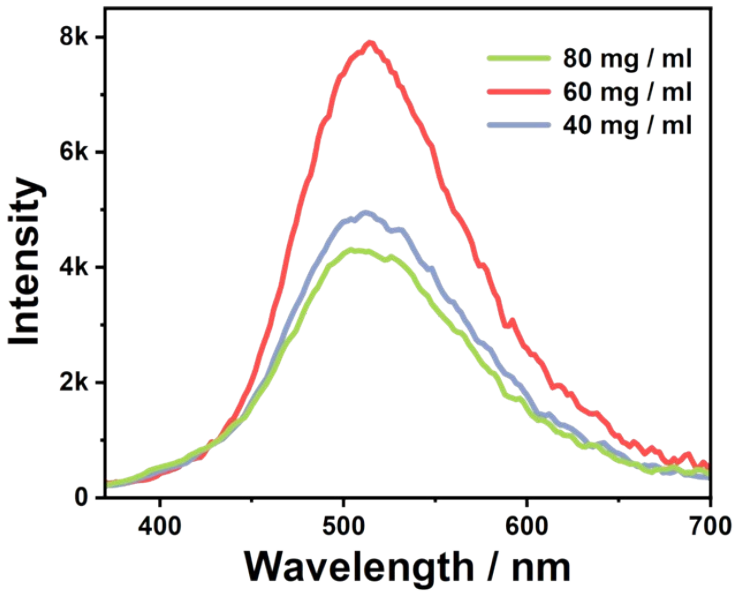

Fig. S13 Phosphorescence intensity excited at 280 nm for ACB-COOH-doped (1 mg/ml) PVA with different concentrations of PVA.

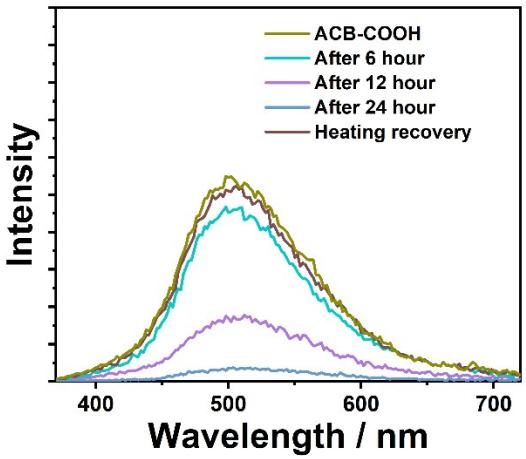

Fig. S14 Phosphorescence emission spectra of ACB-COOH, after swallowing water vapor from the atmosphere for 6, 12, 24 hours, and reheating.

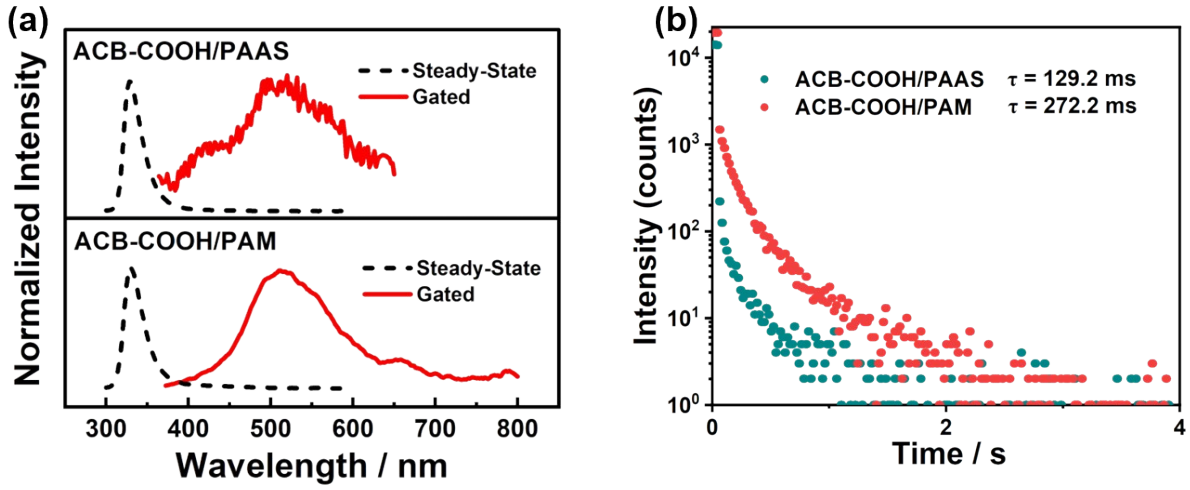

Fig. S15 (a) The normalized steady-state photoluminescence (dash lines) and phosphorescence (solid lines) spectra of ACB-COOH in PAAS and PAM matrix under ambient conditions. (b) Lifetime decay profiles of ACB-COOH in PAAS and PAM matrix monitoring bands at 510 nm.

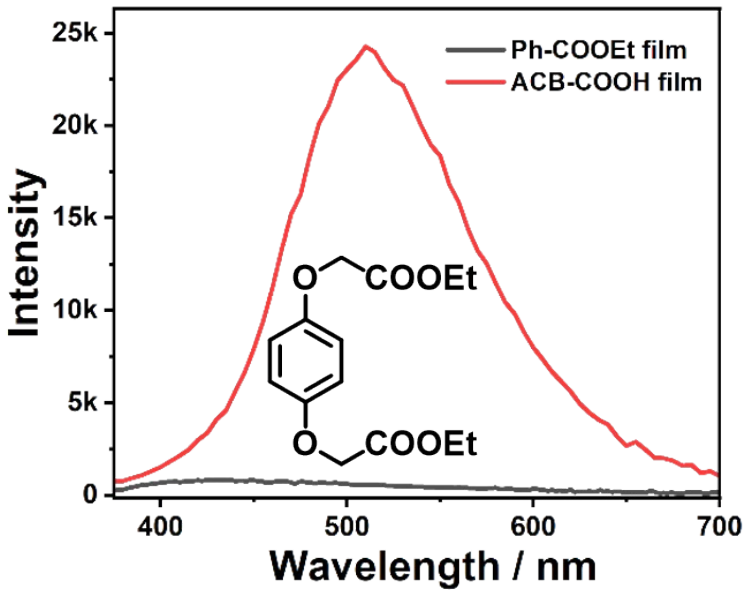

Fig. S16 Phosphorescence emission spectra of Ph-COOEt film and ACB-COOH film.

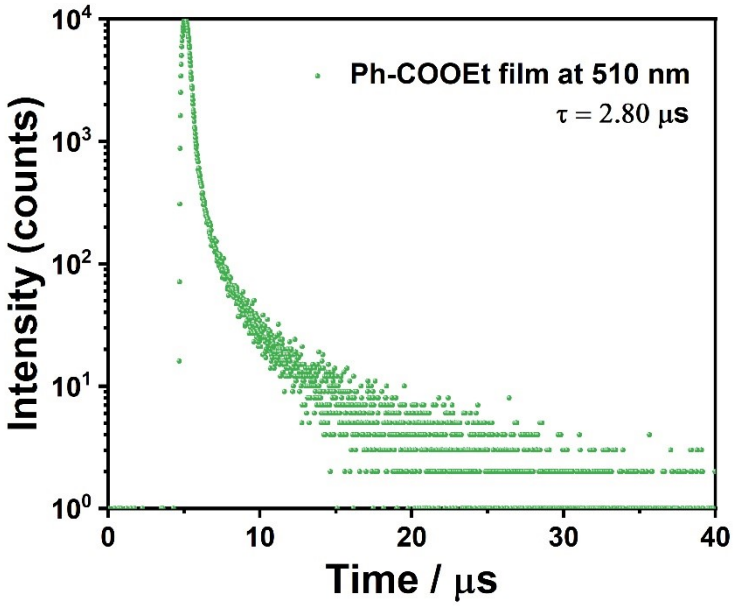

Fig. S17 The time-resolved PL decay spectrum of Ph-COOEt film at 510 nm..

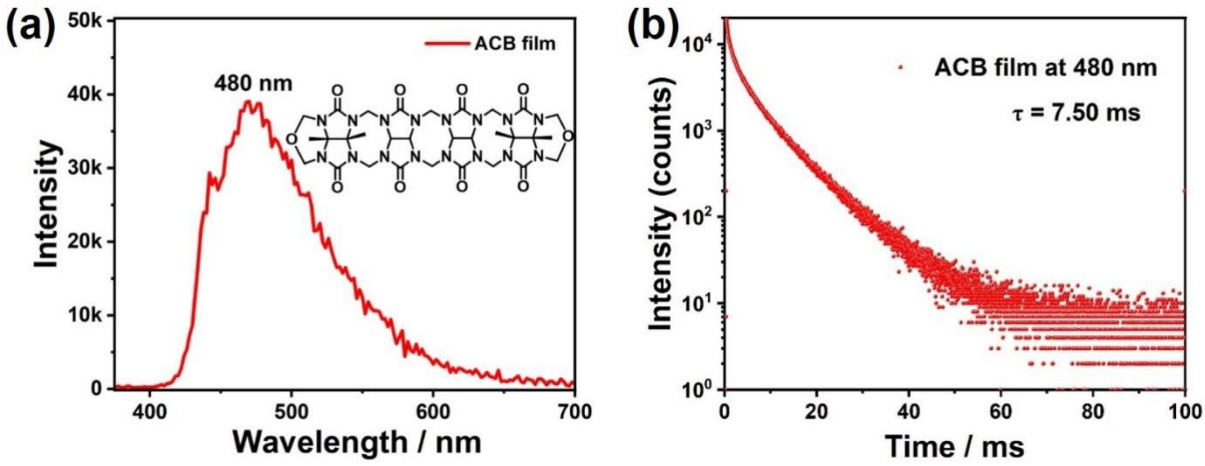

Fig. S18 (a) Phosphorescence emission spectra of ACB film. (b) The time-resolved PL decay spectrum of ACB-doped PVA film at 480 nm.

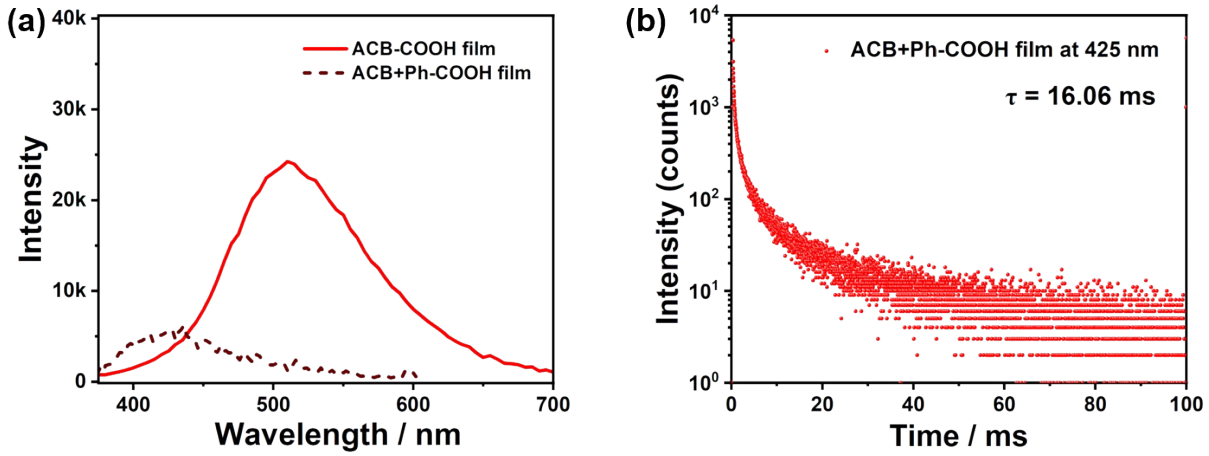

Fig. S19 (a) Phosphorescence emission spectra of ACB+Ph-COOH film and ACB-COOH film. (b) The time-resolved PL decay spectrum of ACB+Ph-COOH film at 425 nm.

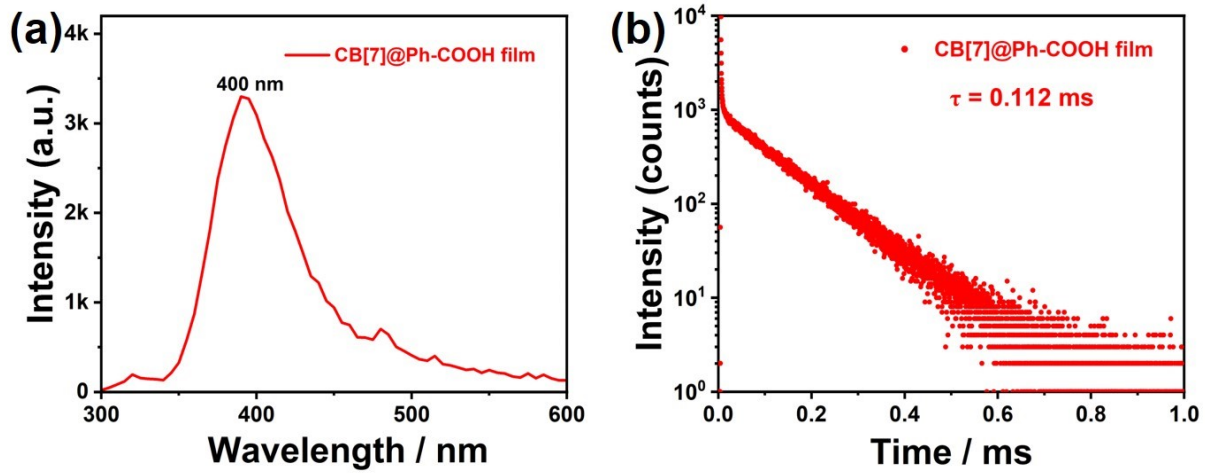

Fig. S20 (a) Phosphorescence emission spectra of CB[7]@Ph-COOH film. (b) The time-resolved PL decay spectrum of CB[7]@Ph-COOH film at 420 nm.

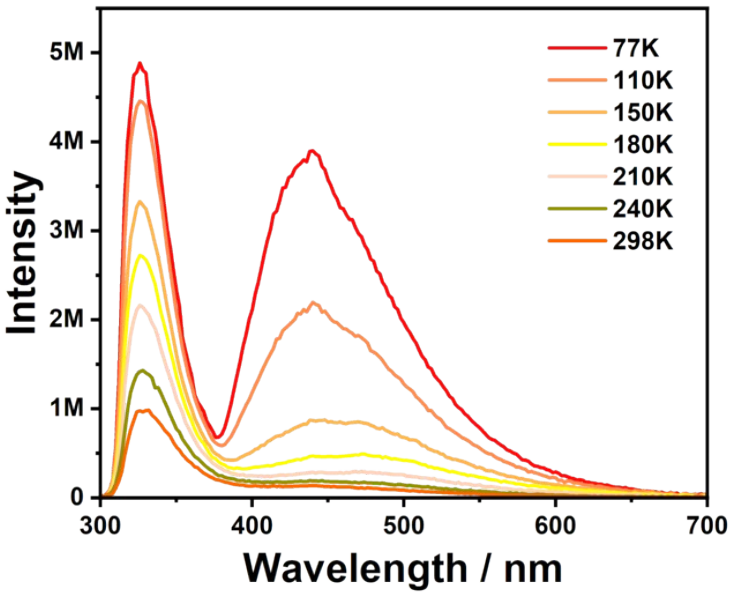

Fig. S21 Temperature-dependent prompt spectra of ACB-COOH powder from 77 to 298 K.

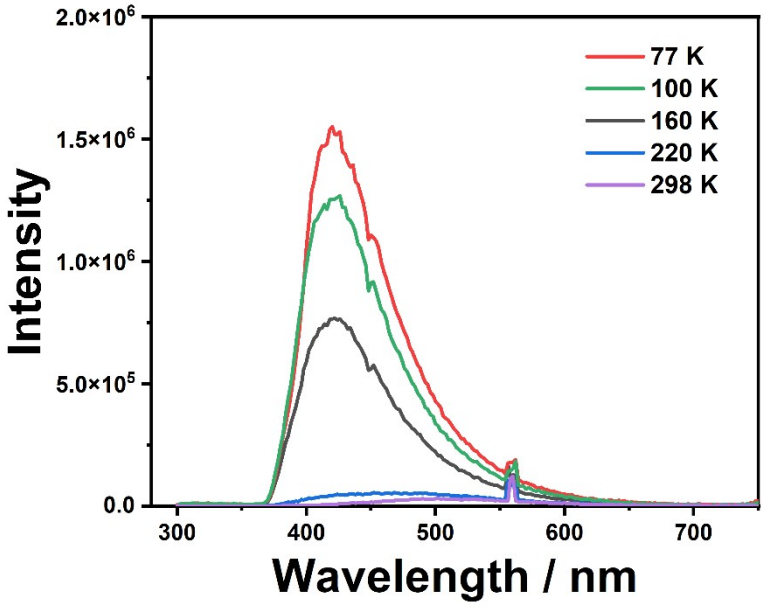

Fig S22. Temperature-dependent delayed (delayed 50 μs) spectra curves of ACB-COOH film (λ_{ex} = 280 nm).

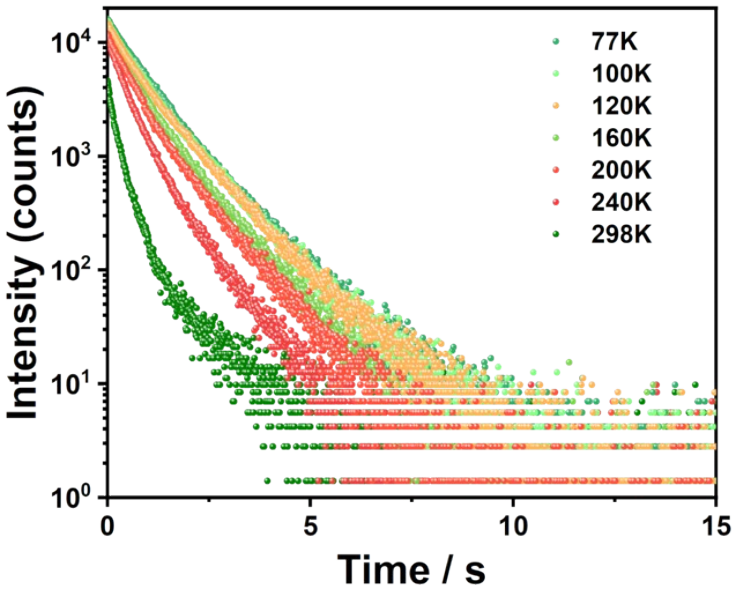

Fig. S23 Temperature-dependent lifetime decay curves of ACB-COOH film from 77 to 298 K.

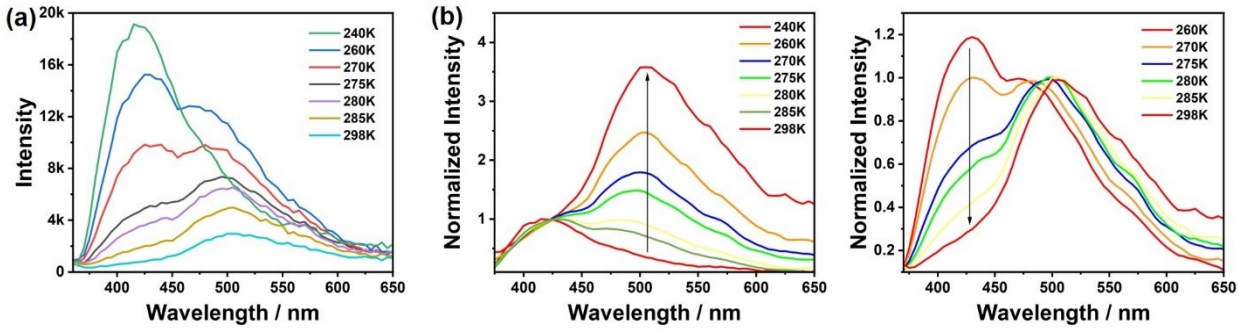

Fig. S24 Normalized temperature-dependent delayed spectra of ACB-COOH film from 240 to 298 K.

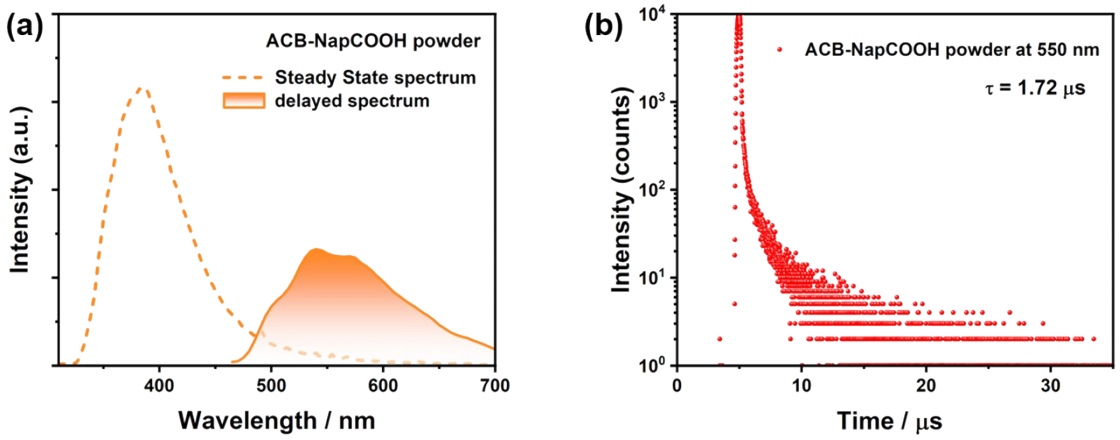

Fig. S25 (a) Photoluminescence emission and phosphorescence emission spectra of ACB-NapCOOH

powder. b) The time-resolved PL decay spectrum of ACB-NapCOOH powder at 550 nm.

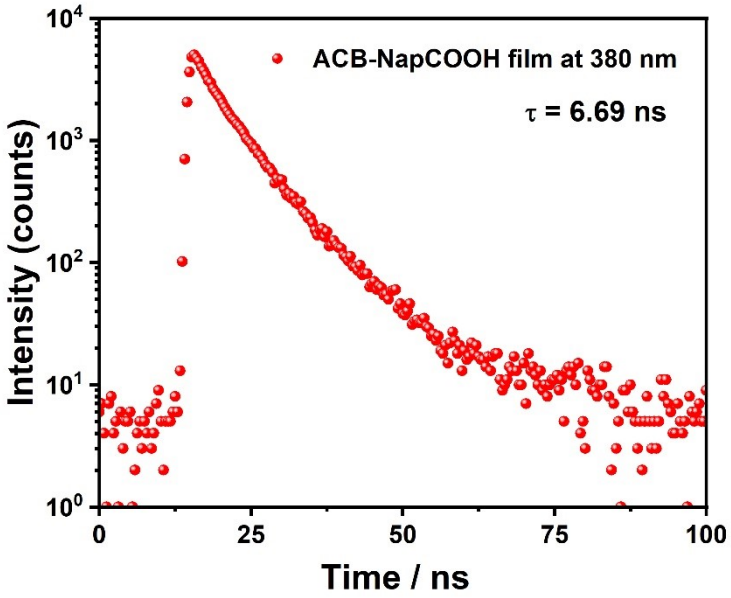

Fig. S26 The time-resolved PL decay curve of ACB-NapCOOH film at 380 nm.

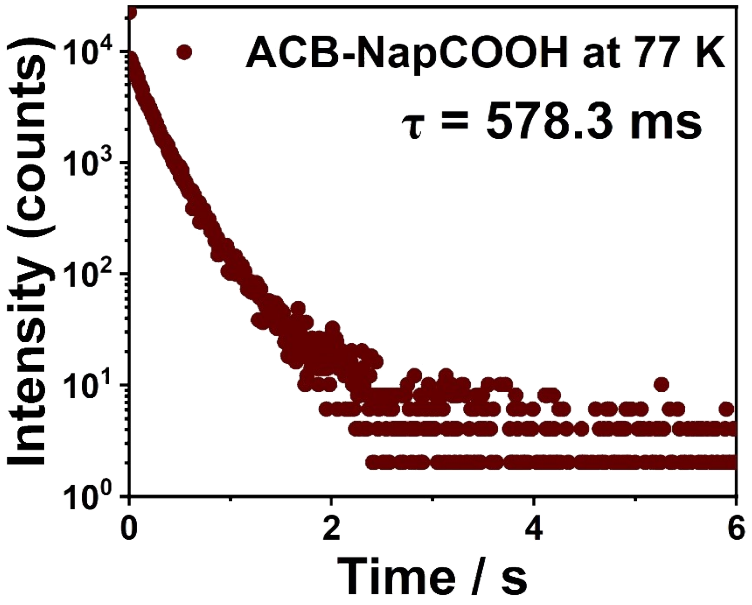

Fig. S27 Phosphorescence lifetime decay curves of ACB-NapCOOH powder at 540 nm at 77 K.

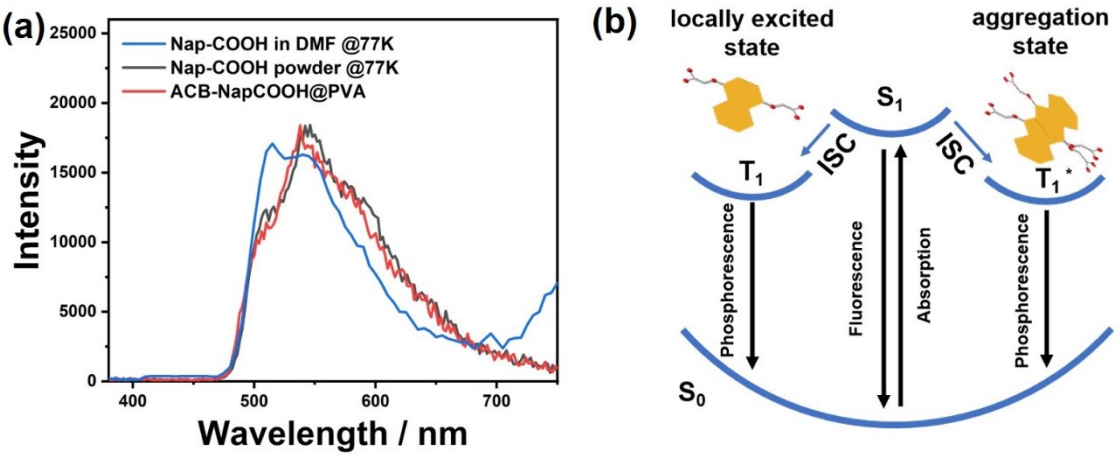

Fig. S28 (a) Normalized phosphorescence spectra of Nap-COOH in DMF, Nap-COOH powder at 77 K and ACB-NapCOOH@PVA at 298 K. (b) Proposed diagram of photophysical process for Nap-COOH.

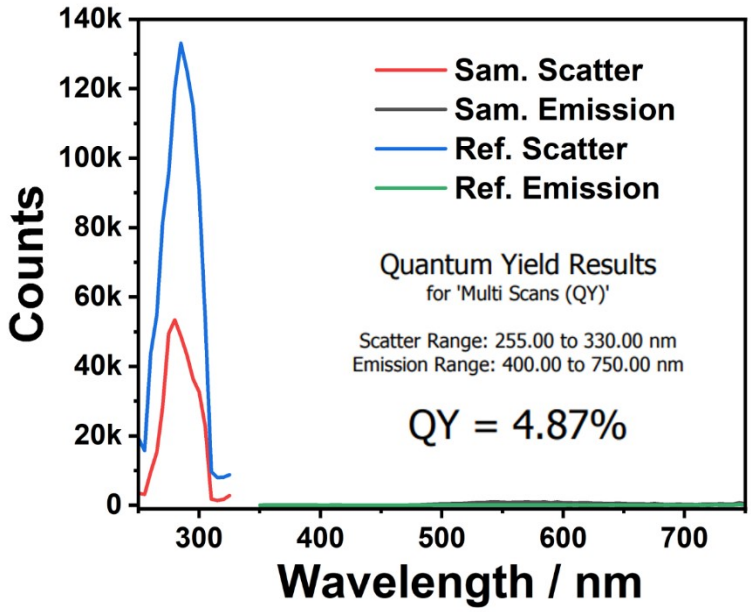

Fig. S29 The quantum yield of ACB-NapCOOH film.

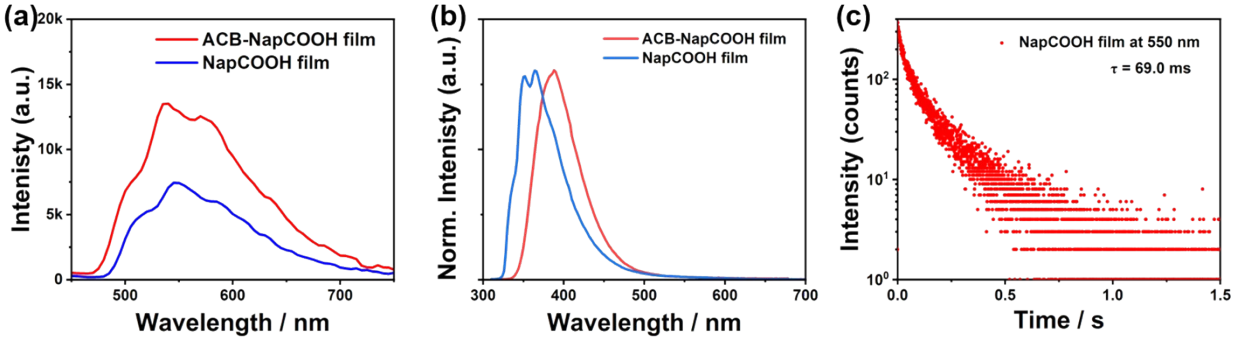

Fig. S30 (a) Phosphorescence emission spectra excited at 310 nm of ACB-NapCOOH film and NapCOOH film. (b) Photoluminescence emission spectra of ACB-NapCOOH film and NapCOOH film. (c) The time-resolved PL decay spectrum of NapCOOH film at 550 nm.

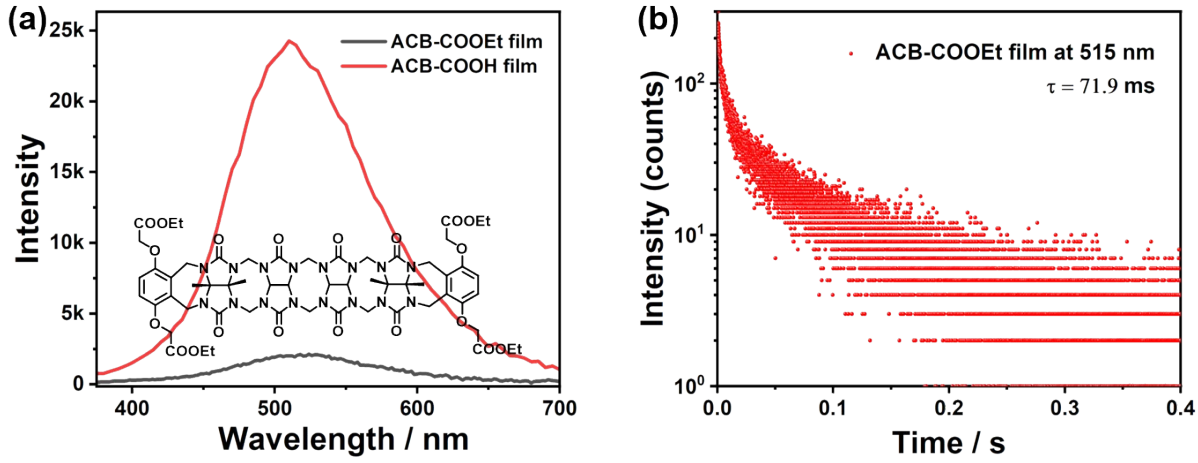

Fig. S31 (a) Phosphorescence emission spectra of ACB-COOEt film and ACB-COOH film. (b) The time-resolved PL decay spectrum of ACB-COOEt film at 515 nm.

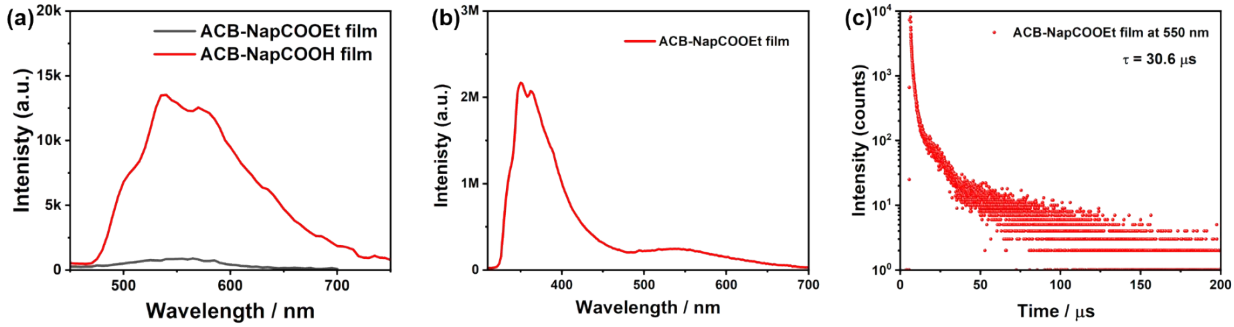

Fig. S32 (a) Phosphorescence emission spectra excited at 310 nm of ACB-NapCOOH film and ACB-NapCOOEt film. (b) Photoluminescence emission spectra of ACB-NapCOOH film and ACB-NapCOOEt film. (c) The time-resolved PL decay spectrum of ACB-NapCOOEt film at 550 nm.

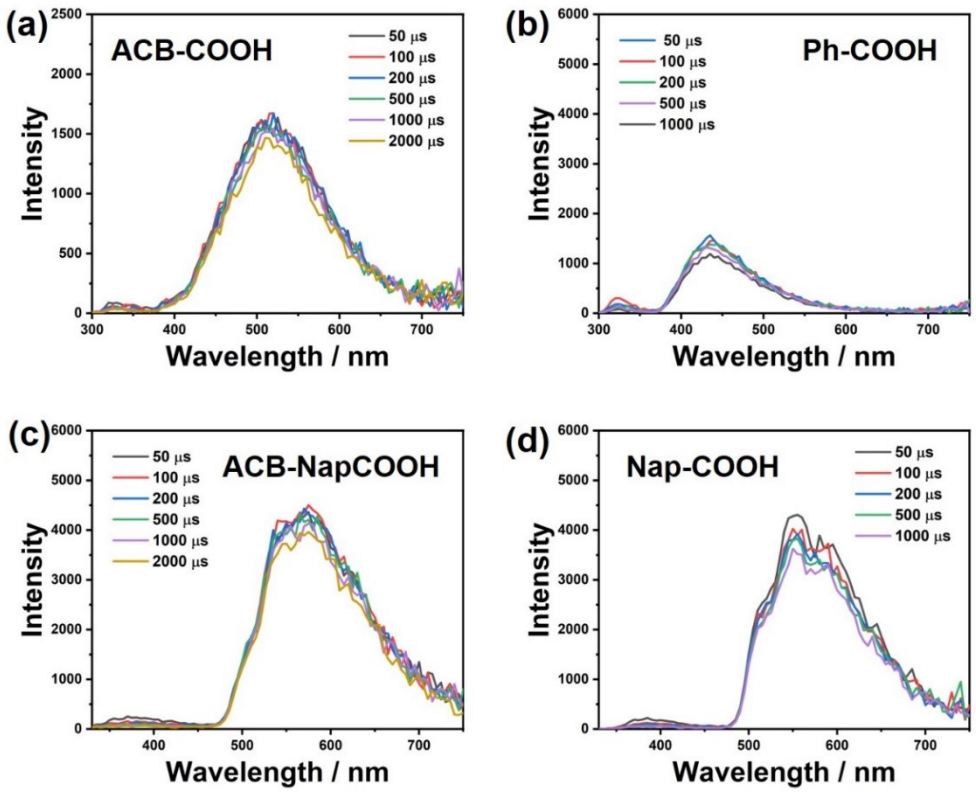

Fig. S33 Delay time-dependent spectra curves of (a) ACB-COOH film, (b) Ph-COOH film, (c) ACB-NapCOOH film and (d) NapCOOH film at 298 K.

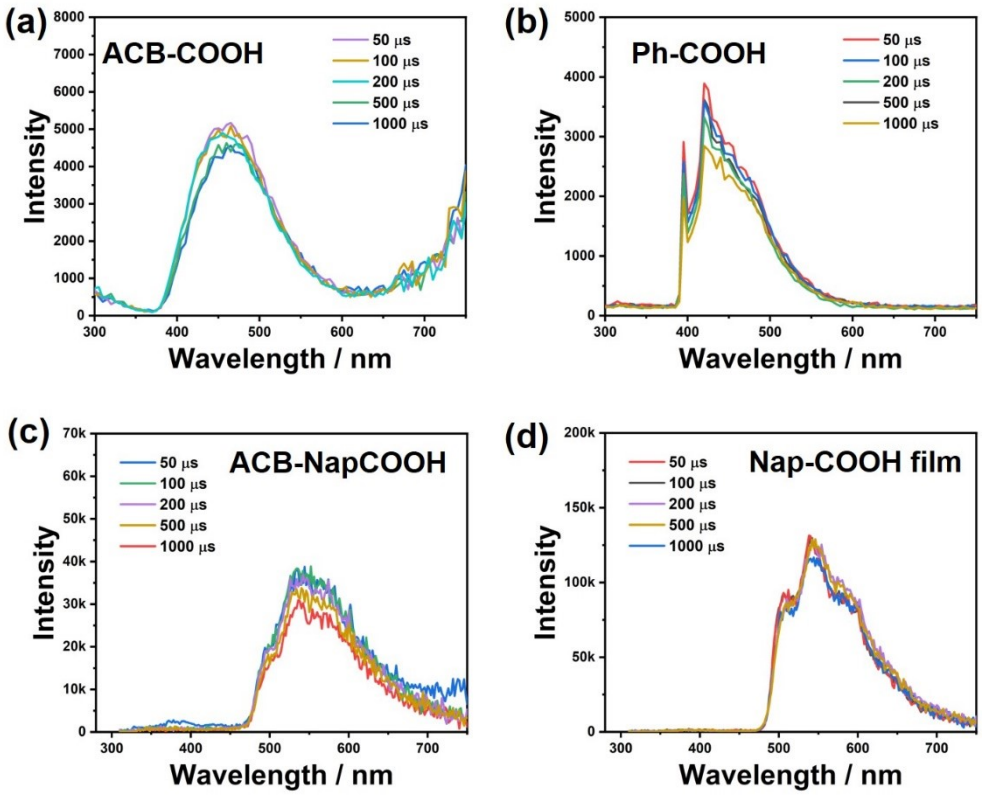

Fig. S34 Delay time-dependent spectra curves of (a) ACB-COOH, (b) Ph-COOH, (c) ACB-NapCOOH and (d) NapCOOH at 77 K.

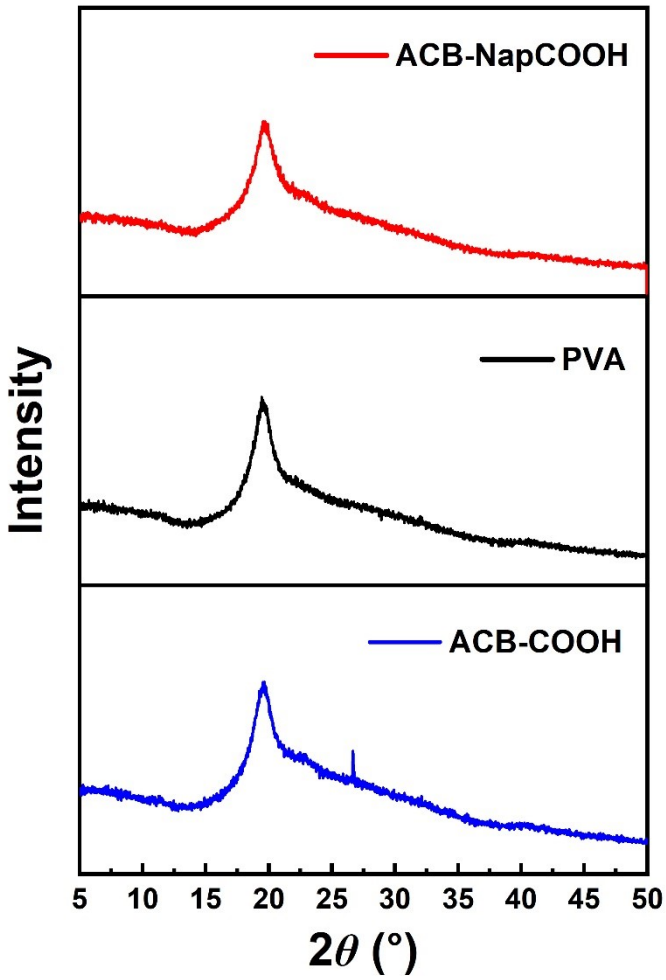

Fig. S35 Experimental XRD patterns of ACB-COOH@PVA, neat PVA and ACB-NapCOOH@PVA films under ambient conditions.

Section D. Host-Guest Properties of ACB-COOH and RhB, PyY or Mor.

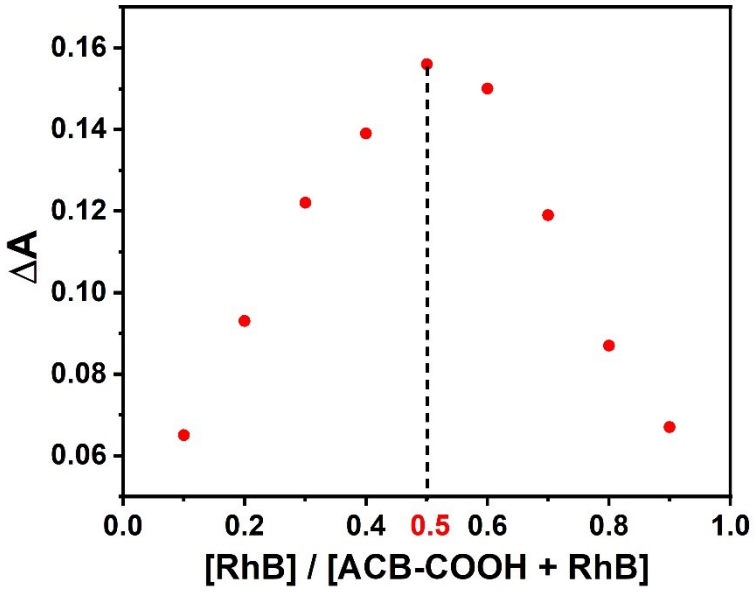

Fig. S36 Job's experiment for RhB upon complexation with ACB-COOH in aqueous solution at 298 K. Absorbance intensity changes of RhB recorded at 548 nm was used to analyze the binding ratio. The total concentration of host and guest is constant ([RhB] + [ACB-COOH] = 1.0×10^{-5} M)

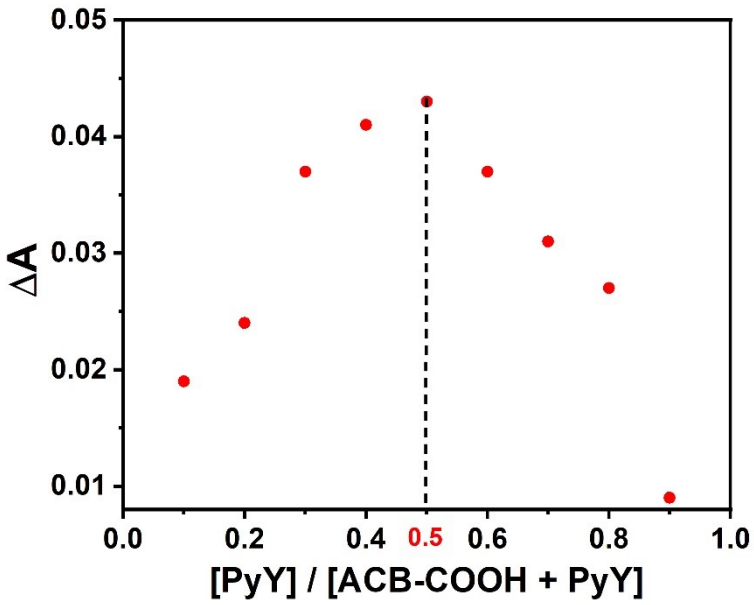

Fig. S37 Job's experiment for PyY upon complexation with ACB-COOH in aqueous solution at 298

K. Absorbance intensity changes of PyY recorded at 540 nm was used to analyze the binding ratio. The total concentration of host and guest is constant ([PyY] + [ACB-COOH] = 1.0×10^{-5} M)

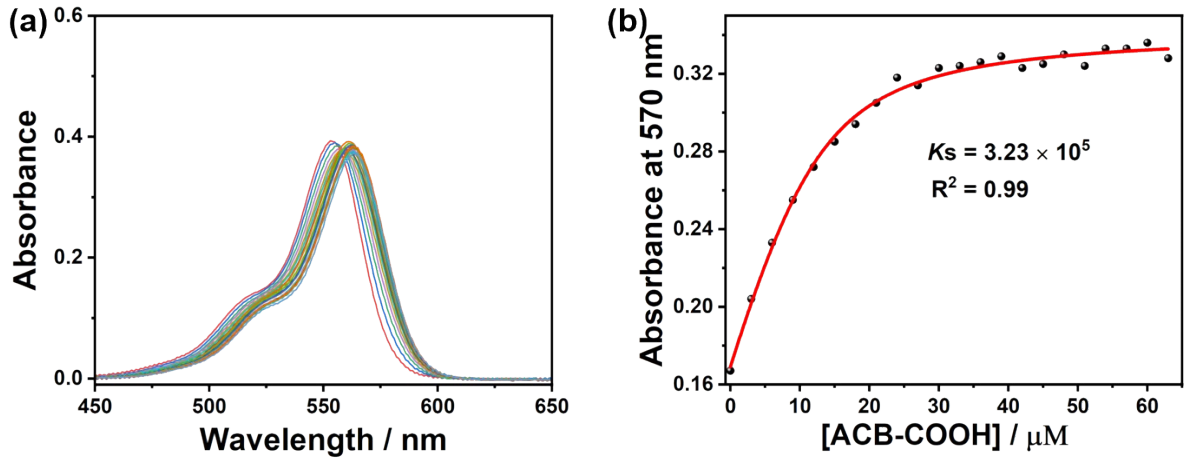

Fig. S38 (a) UV–vis absorption spectra changes of RhB (2.0×10^{-5} M) upon the addition of ACB-COOH in aqueous solution at 298 K. (b) Nonlinear least-squares analysis of the absorbance intensity changes of RhB upon addition of ACB-COOH at 570 nm to calculate the *K*s value between RhB and ACB-COOH ([RhB] = 2.0×10^{-5} M, [ACB-COOH] = 0−6.0×10^{-5} M, 298 K) in aqueous solution.

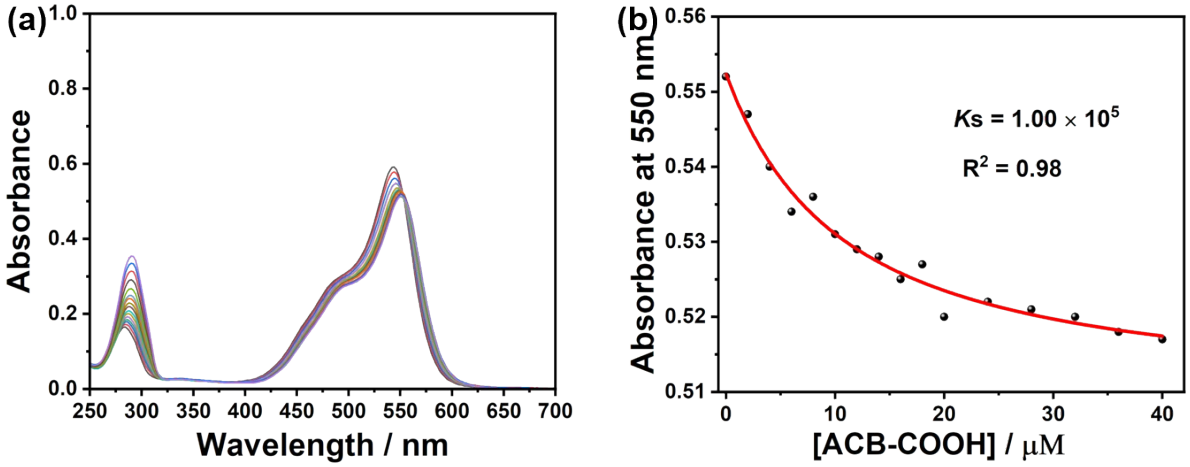

Fig. S39 (a) UV–vis absorption spectra changes of PyY (1.0×10^{-5} M) upon the addition of ACB-COOH in aqueous solution at 298 K. (b) Nonlinear least-squares analysis of the absorbance intensity changes of PyY upon addition of ACB-COOH at 550 nm to calculate the *K*s value between PyY and ACB-COOH ([PyY] = 1.0×10^{-5} M, [ACB-COOH] = 0−4.0×10^{-5} M, 298 K) in aqueous solution.

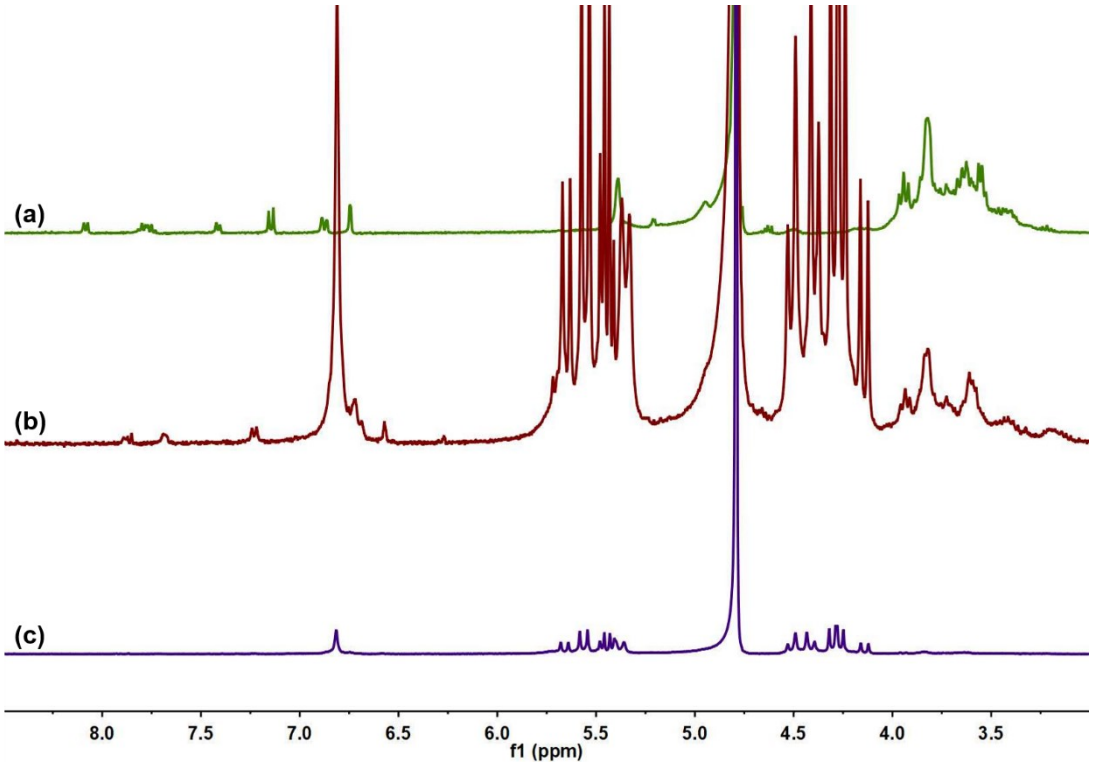

Fig. S40 ^{1}H NMR spectra recorded (600 MHz, RT, D_2O) for a) RhB (0.5 mM), c) ACB-COOH (0.5 mM), b) a mixture of RhB (0.5 mM) and ACB-COOH (2 mM).

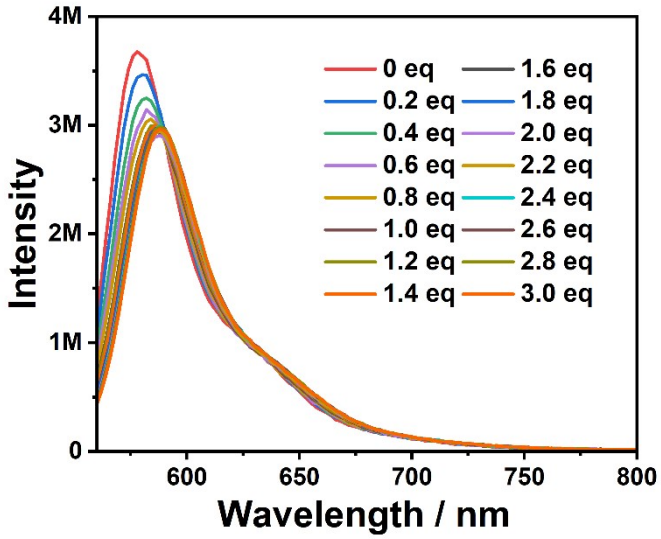

Fig. S41 PL spectra of RhB aqueous solution with different ACB-COOH contents (λ_{ex}=540 nm, [RhB] = 2.0 × 10^{-5} M, [ACB-COOH] = 0−6.0 × 10^{-5} M, 298 K).

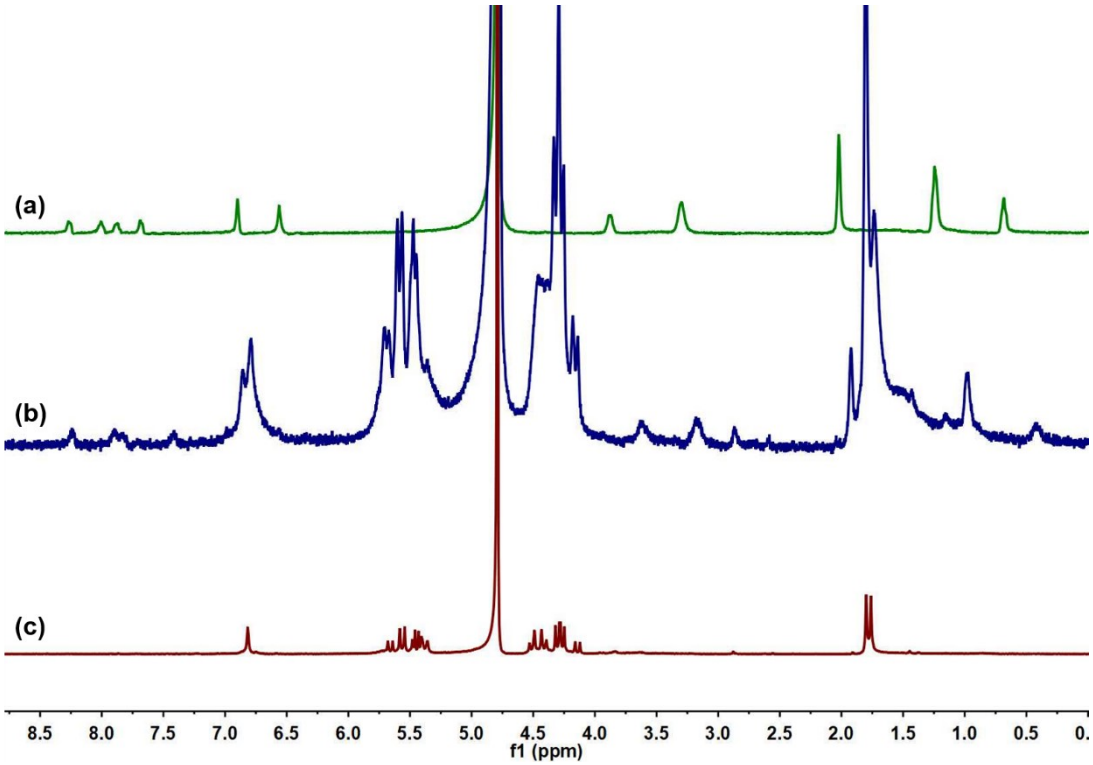

Fig. S42 ^{1}H NMR spectra recorded (600 MHz, RT, D_2O) for a) PyY (0.5 mM), c) ACB-COOH (0.5 mM), b) a mixture of PyY (0.5 mM) and ACB-COOH (2 mM).

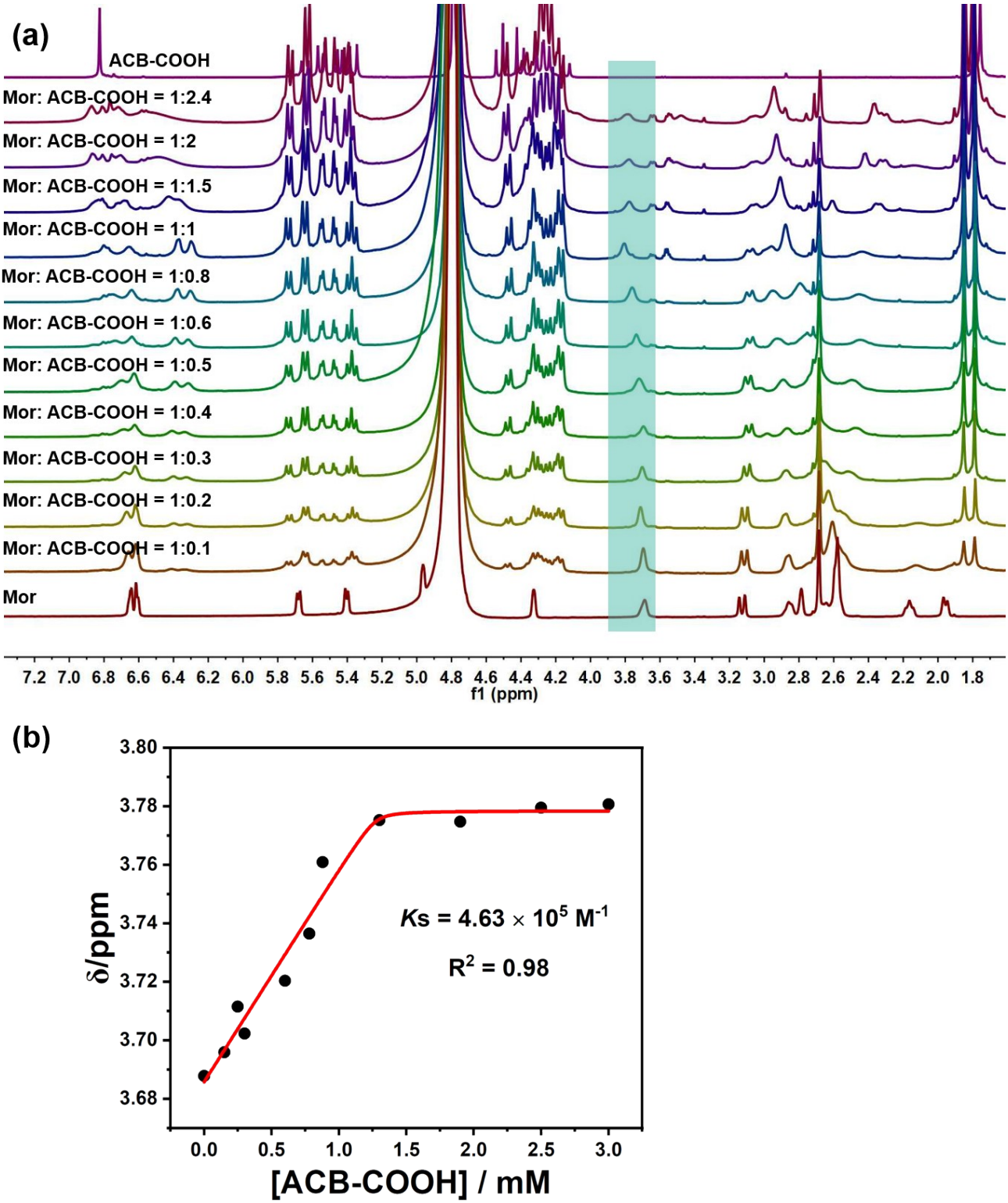

Fig. S43 (a) ^{1}H NMR spectra of Mor (1.25 mM) with 0, 0.125, 0.250, 0.375, 0.500, 0.625, 0.750, 1.000, 1.250, 1.875, 2.5, 3.0 mM ACB-COOH in D_2O at 25 °C. (b) Chemical shift changes of Mor peaks at d = 3.688 ppm vs the concentration of ACB-COOH by using the nonlinear least-squares fitting method.

Section E. Characterizations of photoinduced electron transfer (PET) process of Mor⊂ACB-COOH film.

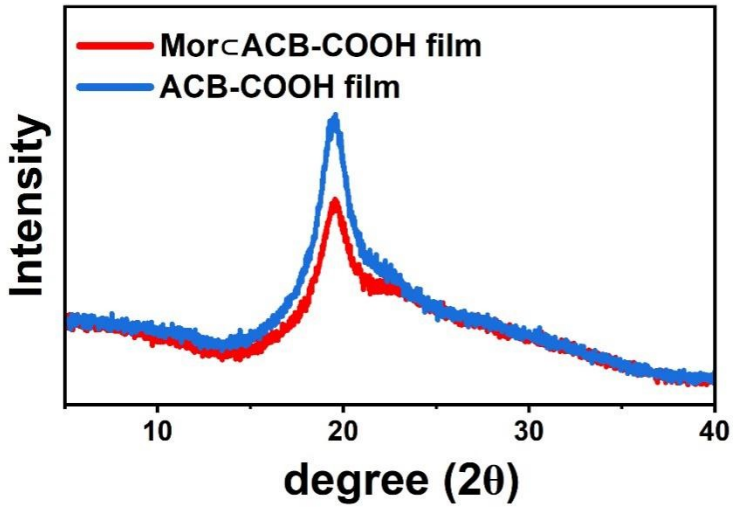

Fig. S44 Experimental XRD patterns of ACB-COOH@PVA, Mor⊂ACB-COOH@PVA films under ambient conditions.

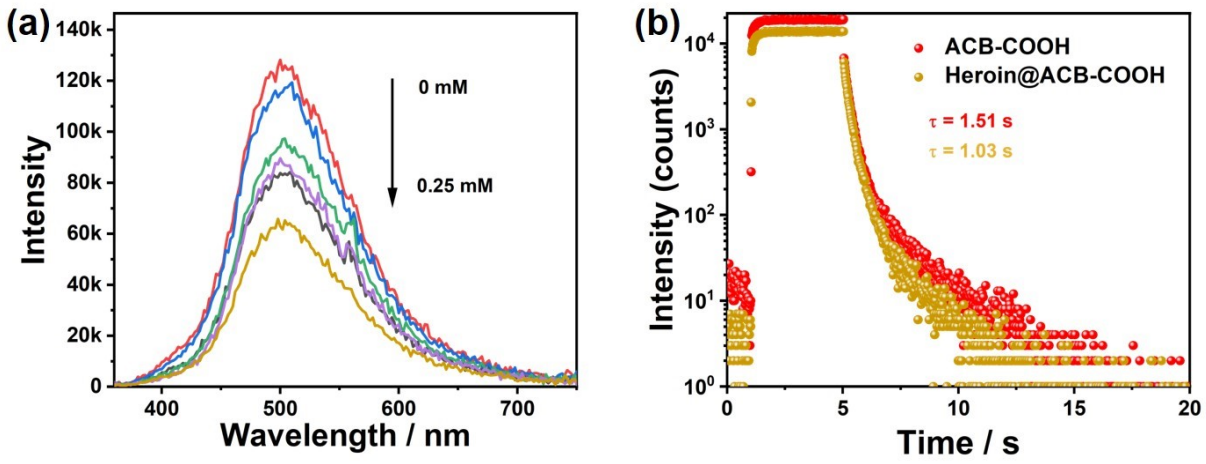

Fig. S45 (a) Phosphorescence emission spectra of ACB-COOH upon incremental addition of Heroin (0-0.25 mM). (b) The phosphorescence lifetime of ACB-COOH film and Heroin⊂ACB-COOH ([Heroin]=0.25 mM) film excited at 280 nm.

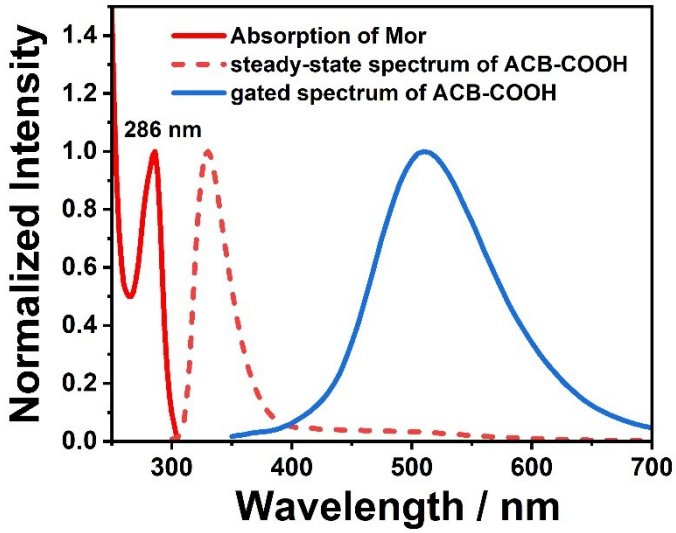

Fig. S46 Absorption spectrum of the Mor and steady-state spectrum and gated spectrum of ACB-COOH films.

Section F. Characterizations of Phosphorescence Energy Transfer Behaviors of RhB⊂ACB-COOH or PyY⊂ACB-COOH film.

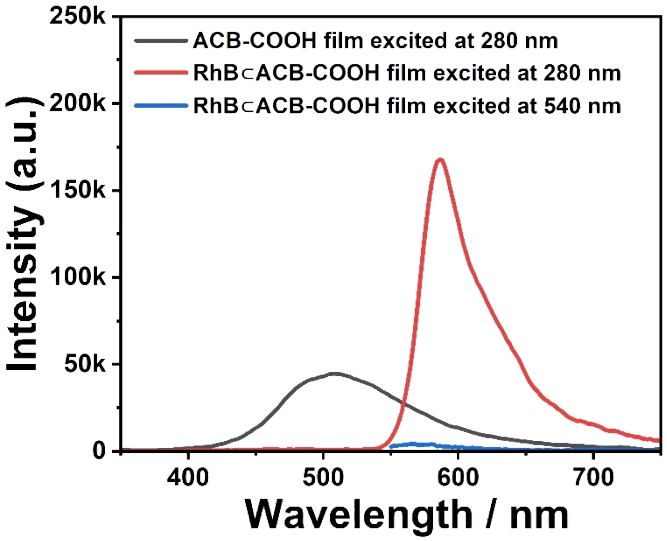

Fig. S47 Phosphorescence emission spectra of ACB-COOH film and RhB⊂ACB-COOH film excited at 280 nm and RhB⊂ACB-COOH film excited at 540 nm.

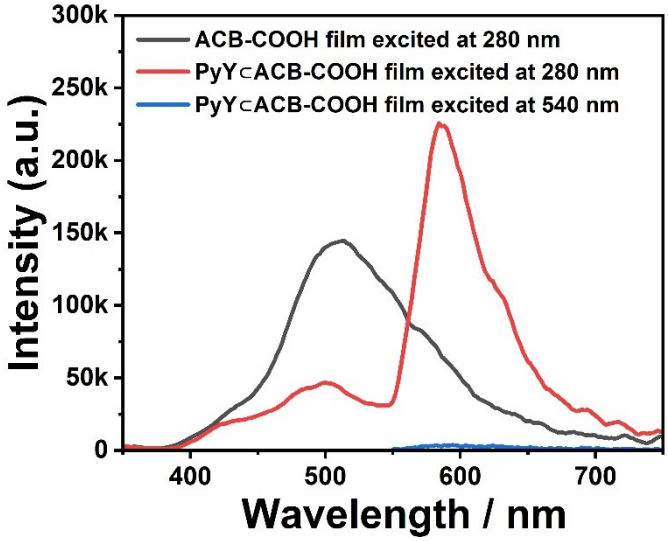

Fig. S48 Phosphorescence emission spectra of ACB-COOH film and PyY⊂ACB-COOH film excited at 280 nm and PyY⊂ACB-COOH film excited at 540 nm.

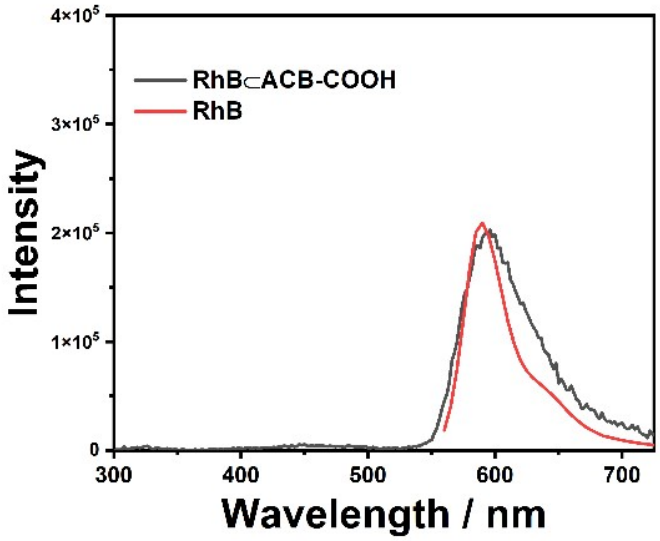

Fig. S49 Normalized delayed emission spectrum (delayed 50 μs) of RhB⊂ACB-COOH@PVA film (λex = 280 nm) and fluorescence emission spectrum of RhB@PVA film (λex = 550 nm).

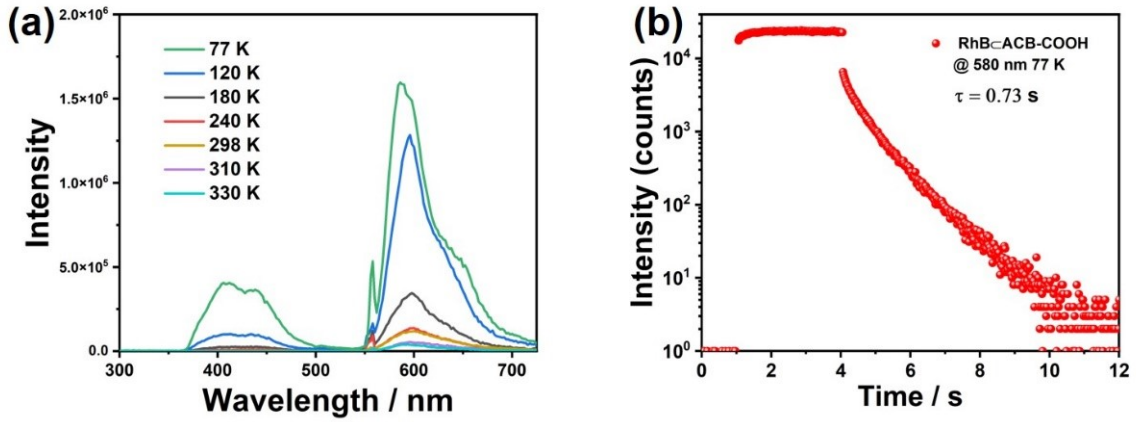

Fig. S50 (a) Temperature-dependent delayed (delayed 50 μs) spectra of RhB⊂ACB-COOH@PVA film from 77 to 330 K (λex = 280 nm). (b) The time-resolved PL decay spectrum of RhB⊂ACB-COOH@PVA film at 580 nm at 77 K.

Section G. Reference:

[1]. Q. Jia, X. Du, C. Wang, K. Meguellati, *Chin. Chem. Lett.* **2019**, *30*, 721-724.

[2]. D. Ma, G. Hettiarachchi, D. Nguyen, B. Zhang, J. B. Wittenberg, P. Y. Zavalij, V. Briken, L. Isaacs, *Nat. Chem.* **2012**, *4*, 503-510.

[3]. D. Ma, P. Y. Zavalij, L. Isaacs, *J. Org. Chem.* **2010**, *75*, 4786-4795.

[4]. S. Jiang, S. Lan, D. Mao, X. Yang, K. Shi, D. Ma, *Chem. Comm.* **2018**, *54*, 9486-9489.